J|A|C|S
COMMUNICATIONS

Published on Web 02/21/2004

Mineralomimetic Sodalite- and Muscovite-Type Coordination Frameworks. Dynamic Crystal-to-Crystal Interconversion Processes Sensitive to Ion Pair Recognition

Elisa Barea,[†] Jorge A. R. Navarro,*[,†] Juan M. Salas,*[,†] Norberto Masciocchi,*[,‡] Simona Galli,[‡] and Angelo Sironi[§]

Departamento de Química Inorgánica, Universidad de Granada, Avenida Fuentenueva S/N, E-18071 Granada, Spain, Dipartimento di Scienze Chimiche, Fisiche e Matematiche, Università degli Studi dell'Insubria, via Valleggio 11, I-22100 Como, Italy, and Dipartimento di Chimica Strutturale e Stereochimica Inorganica, Università di Milano, and ISTM-CNR, via G. Venezian 21, I-20133 Milano, Italy

Received November 7, 2003; E-mail: jarn@ugr.es; jsalas@ugr.es; norberto.masciocchi@uninsubria.it

Since the mid 1990s, a great interest is being directed to the design of extended open metal−organic frameworks (MOFs), which mimic the properties of conventional porous solids[1] and, at the same time, overcome their limitations.[2] Thus, in contrast to aluminosilicates, MOFs can be designed at will[3] to control their shape,[4] functionalization, flexibility,[5] and, additionally, chirality.[6]

In this regard, we are making use of simple diazaaromatic anions to construct extended coordination frameworks with rich structural, thermal, magnetic, and sorptive properties.[7] For instance, we have recently reported a group of neutral and flexible 3D sodalite-type MOFs of formula $[CuL_2]$, with L = 2-pyrimidinolate (2-pymo)[8a] or 4-pyrimidinolate (4-pymo).[8b] The overall structural features are nearly independent of the position of the oxygen atom on the pyrimidine ring, but the shape, size, hydrophilicity, and ion pair affinity of the cavities are highly affected.

While cation and anion recognition processes are clearly understood, more attention is now devoted to ion pair recognition.[9] With this aim, we report hereafter a detailed study of the affinity of the $[Cu(2\text{-pymo})_2]_n$ (**1**) MOF for ion pairs.

The results show that heterogeneous solid−liquid sorption processes are responsible for an unexpected wide variety of guest-induced crystal-to-crystal phase transitions taking place in the MOF host, which are highly dependent on liquid-phase polarity and nature of the guests. Thus, we have found that the sorption selectivity of **1** for ion pairs containing ammonium or alkali cations and "cubic" anions (ClO_4^-, BF_4^-, PF_6^-) from aqueous solution[8a] is extended to a wider range of ion pairs containing D_{3h} NO_3^- anions when the solvent polarity is slightly reduced (MeOH/H_2O or EtOH/H_2O mixtures). Additionally, the novel sorption processes were found to induce profound structural changes in the original $[Cu(2\text{-pymo})_2]_n$ (**1**) MOF (Figure 1).

An ab initio X-ray powder diffraction (XRPD) study on the hydrated $[Cu(2\text{-pymo})_2]_n$ *rhombohedral* material (**1$_R$**) reveals its distorted 3D sodalite-type framework[10] (Figure 1). This 3D framework is not rigid but, upon exposure to an aqueous methanol solution of MNO_3 (M = NH_4, Li), a transition to a *cubic* phase, $[Cu(2\text{-pymo})_2]_n\cdot(MNO_3)_{n/3}$ (**MNO_3@1$_C$**), is observed.[11] Single-crystal X-ray studies performed on the **MNO_3@1$_C$** systems with M = NH_4 and Li[12] show that they contain an undistorted sodalite $[Cu(2\text{-pymo})_2]_n$ MOF (**1$_C$**) with water molecules and $LiNO_3$ or NH_4NO_3 ionic pairs included in the hexagonal channels (Figure 2a). A related structural change from the rhombohedral phase (**1$_R$**) to the cubic one (**1$_C$**) also takes place upon dehydration by heating over 60−70 °C (Figure 3; $\Delta V_m = -35$ Å^3). Both processes are fully reversible; i.e., rehydration of **1$_C$** or MNO_3 removal from **MNO_3@1$_C$** by exposition to water restores **1$_R$**.

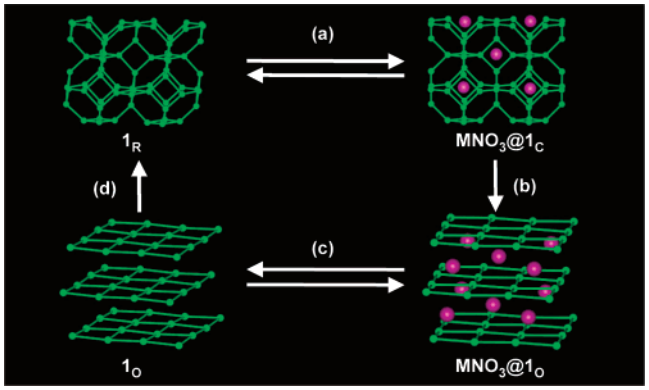

Figure 1. Guest-induced transformations in the $[Cu(2\text{-pymo})_2]_n$ (**1$_R$**) framework: (a) incorporation of $n/3$ MNO_3; (b) additional incorporation of $n/6$ MNO_3; (c) removal of $n/2$ MNO_3; (d) water addition. For M's, see text. Green and purple balls and sticks denote Cu, MNO_3 and 2-pymo-*N*,*N*′-bridges, respectively. Coordinates from the structures of **1$_R$**, **$LiNO_3$@1$_R$**, and **$RbNO_3$@1$_O$**.

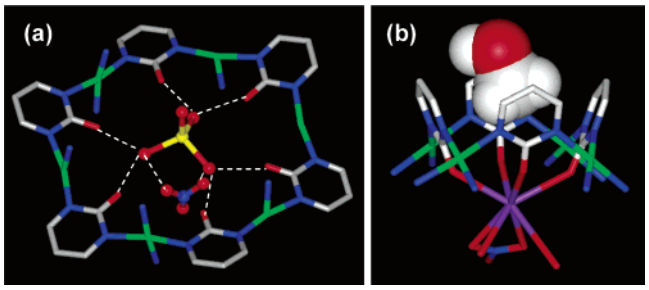

Figure 2. (a) Supramolecular recognition of $[Li(H_2O)_4]NO_3$ in the hexagonal windows of the sodalite β-cages in **$LiNO_3$@1$_C$**. (b) The metallacalix[4]arene motif in **$RbNO_3$@1$_O$**: the lower rim recognizes $RbNO_3(H_2O)$, the cone cavity MeOH. Li (yellow), Rb (purple), Cu (green), O (red), N (blue), C (gray), and H (white).

The reversible process from **1$_R$** to **1$_C$** does not imply any bond-breaking in the MOF but only a slight rearrangement of the sodalite β-cages.[13] Upon incorporation of $n/3$ MNO_3 ion pairs or loss of the water molecules hosted in the lattice cavities, (i) the three crystallographically independent 2-pymo ligands (two of which lie on mirror planes) in *R*-3*m*, slightly shift and become fully equivalent in *Pn*-3*m*, and (ii) the hexagonal windows (Cu···Cu in the 5.34−5.65 Å range) become regular (with Cu···Cu 5.54 Å for **MNO_3@1$_C$** and Cu···Cu 5.34 Å for the evacuated **1$_C$**).

Much more pronounced structural changes take place upon exposure of **1$_R$** to aqueous methanol solutions of nitrate salts of

[†] Universidad de Granada.
[‡] Università degli Studi dell'Insubria.
[§] Università di Milano and ISTM-CNR.

10.1021/ja039472e CCC: $27.50

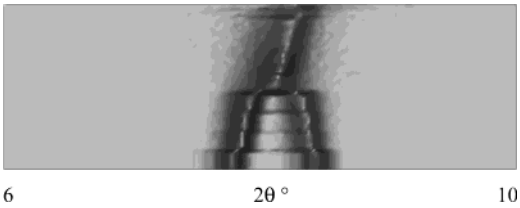

Figure 3. Variable-temperature XRPD traces in the 6−10° 2θ range, showing the progressive merging of the 110 and 012 peaks of $\mathbf{1_R}$ into the 110 reflection of $\mathbf{1_C}$ (a_0 = 15.07 Å). Vertical scale, T in the 25−100 °C range (bottom to top, 10 scans per 10 °C interval). At each T, equilibrium is fully reached. Coalescence occurs at 60 °C.

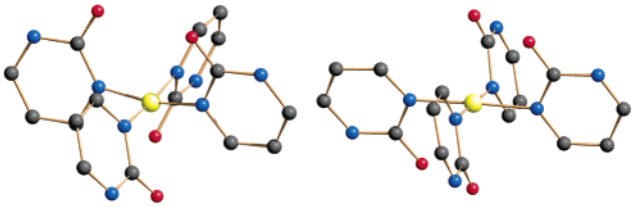

Figure 4. D_{2d} (left) and C_{2h} (right) conformations for the Cu(2-pymo)$_4$ moieties in $\mathbf{1_C}$ and $\mathbf{1_O}$, respectively.

larger cations (Na^+, K^+, Rb^+, Tl^+); the XRPD studies clearly show that the kinetically controlled crystal-to-crystal inclusion process of the 3D framework $\mathbf{1_R}$ to $\mathbf{MNO_3@1_C}$ is, indeed, followed by further incorporation of n/6 MNO_3 ion pairs, leading to a novel series of isomorphous *orthorhombic* layered materials of type $[Cu(2\text{-pymo})_2]_n\cdot(MNO_3)_{n/2}$ ($\mathbf{MNO_3@1_O}$) (Figure 1).

A conventional X-ray study performed on $\mathbf{RbNO_3@1_O}$[14] shows that it consists of square grid $[Cu(2\text{-pymo})_2]_n$ 2D layers (Figure 1), with the Rb^+ ions coordinated to the pyrimidine exocyclic oxygen atoms of the metallacalix[4]arene structural motives (Figure 2b). This feature closely resembles that of a gadolinium-capped complex previously reported by us.[15]

In contrast to the $\mathbf{1_R}$-to-$\mathbf{1_C}$ *displacive* structural phase transition, the process from $\mathbf{1_C}$ to the *layered* $\mathbf{1_O}$ phase implies a complex, *reconstructive* framework reorganization. This solvent-mediated transformation is driven by the templating action of the alkali cations, as found for the formation of discrete metallamacrocycles,[16] and implies (i) a concerted bond-breaking process of the planar sodalite hexagonal windows to square grids and (ii) a reorientation of the pyrimidine ligands from the original D_{2d} conformation of the Cu(2-pymo)$_4$ motives in the $\mathbf{1_C}$ phase to a C_{2h} one in $\mathbf{1_O}$ (Figure 4). These structural changes result in the formation of metallacalix-[4]arene motives in cone conformation, with the heterometals coordinated to the exocyclic pyrimidine oxygens (Figure 2b). Despite the profound guest-promoted structural changes in the host MOF, the *N*,*N*′-bridging mode of the 2-pymo ligand is maintained.

Despite these large guest-induced structural changes, the original $\mathbf{1_R}$ phase can be restored. For instance, refluxing $\mathbf{KNO_3@1_O}$ or $\mathbf{RbNO_3@1_O}$ in MeOH for 6 days with 18-crown-6-ether removes the MNO_3 guests, giving an *empty layered* $[Cu(2\text{-pymo})_2]_n$ species ($\mathbf{1_O}$) which can be readily converted to the original $\mathbf{1_R}$ phase by exposing it to water for a few hours (Figure 1). The reverse structural reorganization from the 2D $\mathbf{1_O}$ to the 3D $\mathbf{1_R}$ MOF implies a swelling of the molar volume of 25 Å^3 due to incorporation of water molecules in the β-cage voids and sodalite channels.

The results presented here show the marked effect of solvent polarity for inducing the pertinent recognition process or structural phase transition. Thus, while metal salts of "cubic" singly charged anions are readily recognized by $\mathbf{1_R}$[8] from water solutions, the related nitrate salts recognition processes take place only in less competitive solvents, such as aqueous MeOH and EtOH, which strengthen the H-bonding acceptor and coordination possibilities of nitrate and pyrimidine oxygens.

The mineralomimetic nature of these systems needs to be highlighted: in addition to the distorted $\mathbf{1_R}$ and undistorted $\mathbf{1_C}$ sodalite frameworks, $\mathbf{1_O}$ can be related to phyllosilicates such as talc (which possesses uncharged layers capable of sorbing neutral "lipophilic" substances) and muscovite (which intercalates metal ions between the negatively charged aluminosilicate layers[17]).

We have further studied the mineralomimetic behavior of $\mathbf{1_R}$ by introducing metal salts of different stoichiometry (Ba^{2+} and La^{3+} nitrates), confirming the tendency of large cations to afford $\mathbf{1_O}$-like phases more or less swollen, with a axes (perpendicular to the $\mathbf{1_O}$ layers) of 18.40 (Na^+), 18.48 (K^+), 18.63 (hydrated $\mathbf{1_O}$), 18.64 (Rb^+), 18.80 (La^{3+}), 18.88 (Tl^+), and 19.20 Å (Ba^{2+}). Work is in progress to obtain new extended systems containing other transition metals.

Acknowledgment. Spanish MCYT (BQU2001-2955-CO2-01, HI2003-0081), MECD (E.B. FPU grant), FPC-Como and Uninsubria (Progetto Sistemi Poliazotati) are acknowledged for funding; A. Kern and A. Coelho (Bruker AXS) are thanked for providing TOPAS (β-version).

Supporting Information Available: Preparation methods and analytical data of the clathrates; packing diagrams of $\mathbf{1_R}$, $\mathbf{NH_4NO_3@1_C}$, $\mathbf{LiNO_3@1_C}$ and $\mathbf{RbNO_3@1_O}$. X-ray crystallographic data, in CIF format, are also provided. This material is available free of charge via the Internet at http://pubs.acs.org.

References

(1) Corma, A. *Chem. Rev.* **1997**, *97*, 2373.
(2) See, e.g.: (a) Yaghi, O. M.; O'Keeffe, M.; Ockwig, N. W.; Chae, H. K.; Eddaoudi, M.; Kim, J. *Nature* **2003**, *423*, 705. (b) Janiak, C. *Dalton Trans.* **2003**, 2781. (c) James, S. L. *Chem. Soc. Rev.* **2003**, *32*, 276.
(3) Eddaoudi, M.; Kim, J.; Rosi, N.; Vodak, D.; Wachter, J.; O'Keefe, M.; Yaghi, O. M. *Science* **2002**, *295*, 469.
(4) Keller, S. W.; Lopez, S. *J. Am. Chem. Soc.* **1999**, *121*, 6306.
(5) Kitaura, R.; Seki, K.; Akiyama, G.; Kitagawa, S. *Angew. Chem., Int. Ed.* **2003**, *42*, 428.
(6) (a) Seo, J. S.; Whang, D.; Lee, H.; Jun, S. I.; Oh, J.; Jeon, Y. J.; Kim, K. *Nature* **2000**, *404*, 982. (b) Lee, S. J.; Lin, W. *J. Am. Chem. Soc.* **2002**, *124*, 4554.
(7) Masciocchi, N.; Ardizzoia, G. A.; La Monica, G.; Maspero, A.; Sironi, A. *Eur. J. Inorg. Chem.* **2000**, 2507. Masciocchi, N.; Bruni, S.; Cariati, E.; Cariati, F.; Galli, S.; Sironi, A. *Inorg. Chem.* **2001**, *40*, 5897. Masciocchi, N.; Galli, S.; Sironi, A.; Barea, E.; Navarro, J. A. R.; Salas, J. M.; Tabares, L. C. *Chem. Mater.* **2003**, *15*, 2153.
(8) (a) Tabares, L. C.; Navarro, J. A. R.; Salas, J. M. *J. Am. Chem. Soc.* **2001**, *123*, 383. (b) Barea, E.; Navarro, J. A. R.; Salas, J. M.; Masciocchi, N.; Galli, S.; Sironi, A. *Polyhedron* **2003**, *22*, 3051.
(9) (a) Piotrowski, H.; Severin, K.; *Proc. Natl. Acad. Sci. U.S.A.* **2002**, *99*, 4997. (b) Bartoli, S.; Roelens, S. *J. Am. Chem. Soc.* **2002**, *124*, 8307.
(10) Crystal data for $\mathbf{1_R}$, $C_8H_8CuN_4O_3$: FW 271.72 g mol^{-1}, trigonal, *R*-3*m*, a = 23.040(2) Å, c = 25.140(2) Å, V = 11.558(2) Å^3, Z = 36, ρ = 1.405 g cm^{-3}, R_{wp}, R_p, and R_{Bragg} = 0.057, 0.043, and 0.022 for 3150 data collected in the 7−70° 2θ range. CCDC no. 223570.
(11) Apart from the evacuated $\mathbf{1_C}$ species, all species host, in their MOF channels, a number of water molecules.
(12) Crystal data for $NH_4NO_3@\mathbf{1_C}$, $C_{24}H_{28}Cu_3N_{14}O_{12}$: FW 895.22 g mol^{-1}, cubic, *Pn*-3*m*, a = 15.6702(5) Å, V = 3847.9(2) Å^3, Z = 4, ρ = 1.545 g cm^{-3}, R = 0.081. Crystal data for $LiNO_3@\mathbf{1_C}$, $C_{24}H_{28}Cu_3LiN_{13}O_{14}$: FW 920.15 g mol^{-1}, cubic, *Pn*-3*m*, a = 15.6475(5) Å, V = 3831.2(2) Å^3, Z = 4, ρ = 1.595 g cm^{-3}, R, 0.063. CCDC nos. 223568 and 223567.
(13) The $\mathbf{1_R}$ and $\mathbf{1_C}$ lattices are related by the $a_R = -b_C - c_C$, $b_R = a_C + c_C$, and $c_R = -a_C - b_C + c_C$ transformations; ideally, for a cubic lattice in rhombohedral description, $c_R/a_R = \sqrt{3}/\sqrt{2} = 1.224$; in the present case, $c_R/a_R = 1.091$.
(14) Crystal data for $RbNO_3@\mathbf{1_O}$, $C_{17}H_{18}Cu_2RbN_9O_9$: FW 704.97 g mol^{-1}, orthorhombic, *Pna*2$_1$, a = 18.783(2) Å, b = 11.020(1) Å, c = 11.450(1) Å, V = 2370.0(4) Å^3, Z = 4, ρ = 2.026 g cm^{-3}, R = 0.063. CCDC no. 223569.
(15) Navarro, J. A. R.; Salas, J. M. *Chem. Commun.* **2000**, 235.
(16) (a) Pecoraro, V. L.; Stemmler, A. L.; Gibney, B. R.; Bodwin, J. J.; Wang, H.; Kampf, J. W.; Barwinski, A. *Prog. Inorg. Chem.* **1997**, *45*, 83. (b) Saalfrank, R. W.; Uller, E.; Demleitner, D.; Bernt, I. *Struct. Bonding (Berlin)* **2000**, *96*, 149.
(17) Putnis, A. *Introduction to Mineral Sciences*; Cambridge University Press: Cambridge, 1992.

JA039472E